RSC Advances

PAPER

View Article Online
View Journal | View Issue

Cite this: *RSC Adv.*, 2019, **9**, 40883

Effects of the aspect ratio of the conductive agent on the kinetic properties of lithium ion batteries†

Hyeonjun Song,‡[a] Yeonjae Oh,‡[a] Nilüfer Çakmakçı[b] and Youngjin Jeong *[ab]

We fabricated lithium-ion batteries (LIBs) using the Super P and carbon nanotubes (CNTs) as conductive agents to investigate the effect of the aspect ratio of conductive agent on the kinetic properties of LIB. The electrode fabricated with CNTs, which have a high aspect ratio (length: 200 μm), exhibited outstanding rate capability at 30C despite of their low concentration, while the electrode fabricated with the carbon black showed poor rate capability. These results indicate that the aspect ratio of conductive agent influence the diffusion coefficient of lithium ions, which is calculated from the galvanostatic intermittent titration technique analysis, and that conductive agent should have high aspect ratio to improve the kinetic properties of LIBs. This study provides insights that are useful for designing high-performance LIBs by reducing the amount of conductive agent, leading to increased loading of active material.

Received 18th November 2019
Accepted 3rd December 2019

DOI: 10.1039/c9ra09609d

rsc.li/rsc-advances

1. Introduction

Lithium-ion batteries (LIBs) are considered as the most preferred power source these days for portable electric devices and electric vehicles (EVs).[1–3] However, the current energy density (150–200 W h kg^{-1}) and power density (250–340 W kg^{-1}) of LIBs less meet the performance required by portable electric devices and EVs.[4–6] Regarding this issue, much research is being carried out to improve the performance of LIBs in terms the energy density and power density by designing the LIB's internal structure and developing new active materials.[6–10]

Due to the typical structure of LIBs, the performance of LIB dominantly depends on these main components which are electrodes, separators, and electrolytes.[11] Practically, the performance of LIB is enhanced by improving the electrodes, which is an essential component of battery and stores Li-ions in LIBs. Generally, the electrodes are prepared by casting slurry which consists of the active materials, a conductive agent, and a polymeric binder, onto a metallic current collector. Because the polymeric binder is an insulator, the conductive agent, which makes the electrode conductive and transfers electrons to the active materials, plays a key role in storing the Li-ions in the active materials. Notably, the conductive agent for cathode has a greater impact on the performance of LIBs because of the low electric conductivity of metal oxide-based cathode material compared to carbon-based anode material.[12,13]

To increase the energy density of LIBs, the loading amount of the active materials is required to be increased. However, an increase in the active material results in an increase in the thickness of the electrode, which in turn increases the internal resistance of the electrode, and thus a decreases the battery performance.[14–16] Carbon black is a commonly used conductive agent to reduce the internal resistance of the electrode; however, it is disadvantageous because of 0D material characteristics. On the other hand, carbon nanotubes (CNTs) are promising material as a conductive agent for reducing the electrode's internal resistance due to their high aspect ratio.[17–19] There are many studies on using CNTs as a conductive agent.[20–23] Nevertheless, the effect of the length of CNTs on the kinetic properties of the battery has not been clarified.

To understand the effect of CNT on LIBs, we investigated the kinetic properties of LIB according to the aspect ratio of CNTs. In the meantime, the $LiCoO_2$ (LCO) half-cell was assembled with carbon black and CNTs of different lengths and electrochemical analyses was conducted.

2. Experimental

2.1 Preparation of electrodes

The CNT film was prepared using the direct spinning method.[24] The precursor solution was consisting of acetone (98.0 wt%, Samchun Chemical, Korea), ferrocene (0.2 wt%, Sigma Aldrich), thiophene (0.8 wt%, ≥99%, Sigma Aldrich), and polysorbate_20 (1.0 wt%, Sigma Aldrich) and the injection was done at a rate of 10 ml h^{-1} into 1200 °C of a vertical reactor with H_2 gas (carrier gas, 1000 sccm).[24] To prepare the slurry for electrode, LCO (MTI

[a]*Department of Information Communication, Materials, and Chemistry Convergence Technology, Soongsil University, Seoul 156-743, Korea. E-mail: yjeong@ssu.ac.kr; Tel: +82-2-820-0667*

[b]*Department of Organic Materials and Fiber Engineering, Soongsil University, Seoul 156-743, Korea*

† Electronic supplementary information (ESI) available. See DOI: 10.1039/c9ra09609d

‡ Hyeonjun Song and Yeonjae Oh contributed equally to this work.

Korea), carbon black (Super P, MTI Korea), and poly(vinylidene difluoride) (PVDF, MTI Korea) were mixed in *N*-methyl-2-pyrrolidone (NMP, Samchun Chemical, Korea) solvent at a weight ratio of 8 : 1 : 1. Further, LCO, CNT (length: 20–30 μm, JEIO, Korea), and PVDF were mixed in NMP solvent at a weight ratio of 8.6 : 0.4 : 1. LCO, CNT (length: 200–300 μm, JEIO), and PVDF were mixed in NMP solvent at a weight ratio of 8.6 : 0.4 : 1. The CNT films were coated with the electrode slurries followed by drying at 120 °C for 2 h in a vacuum oven. The electrodes prepared using the Super P, normal CNT (having length in the range of 20–30 μm), and long CNT (having length in the range of 200–300 μm) were named as SP, NCNT, and LCNT, respectively.

2.2 Fabrication of half-cells

A coin-type half-cell (CR 2032, MTI Korea) was assembled to evaluate the performance of the battery consisted of the prepared electrodes. The prepared electrode and Li metal were used as the working electrode and counter/reference electrode, respectively. Celgard 2325 and a mixture of 1 M $LiPF_6$ dissolved in ethylene carbonate/diethylene carbonate (1 : 1 by volume) were used as the separator and electrolyte, respectively. All the procedures were conducted in an argon-filled glove box (Kiyon, Korea).

2.3 Characterization

Field emission scanning electron microscopy (Carl Zeiss, SIGMA) was used for the morphological analysis of the prepared electrodes. Galvanostatic charge/discharge tests were conducted in 2.8–4.2 V using charge/discharge cycler (Shin Corporation, Japan). AC impedance tests were conducted using the electrochemical impedance spectroscopy (Autolab, PGSTAT 302N) in the frequency range of 10 mHz to 0.1 MHz with an AC voltage amplitude of 10 mV. For the galvanostatic intermittent titration technique (GITT) analysis, the cells were charged with a constant current flux for a given time followed by an open-circuit stand for a specified time interval.

3. Results and discussion

3.1 Morphological analysis

The SEM image of CNT film, which is prepared by direct sinning method in Fig. S1† and it serves as a current collector. The long CNT bundles are entangled and form a network structure as shown in Fig. S1.† Also, rough surface of the CNT film makes a robust adhesion between the CNT film and active materials.[26]

The SEM images of electrodes prepared using Super P as a conductive agent and CNTs are shown in Fig. 1. Fig. 1a and d shows the surface of electrode prepared by using Super P, which shows that the LCO particles were covered with lots of Super P particles. Further, more the Super P was observed in the FEM images than CNTs shown in Fig. 1b and c. This is because the Super P was used 2.5 times more than CNTs. CNTs cover LCOs well, although the amount used is much less than the Super P (Fig. 1e and f). The electrical connection between the active materials and the conductive agents should be well established in order to reduce the internal resistance of the electrode.[25] In order to achieve effective electron, transfer with carbon black, a large amount of Super P (a low aspect ratio) is required (Fig. 1d). Using a large amount of conductive agents will reduce the loading amount of active material and consequently reduce the energy density of the electrode. Despite the use of a low amount of CNT (approximately 40% of Super P), the electrical connectivity between LCOs is well established which is due to the large aspect ratio of CNTs (Fig. 1e and f).

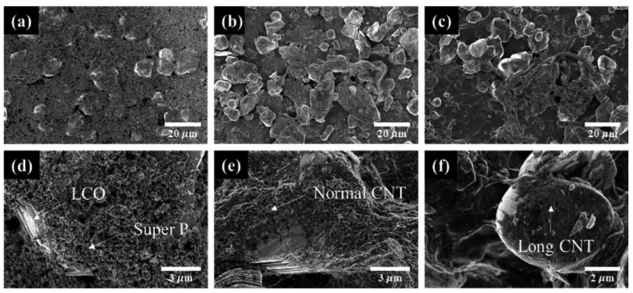

Fig. 1 SEM images of surface of electrode using various conductive agent. (a) SP0, (b) NCNT, and (c) LCNT and magnified view of (d) SP, (e) NCNT, and (f) LCNT.

3.2 Electrochemical analysis

The galvanostatic charge–discharge tests were carried out to evaluate the electrochemical performance of the electrodes (Fig. 2). The shape of voltage profiles indicates that the cells fabricated with the electrodes work well, despite the difference in the content of the conductive agent (Fig. 2a–c). The initial discharge capacities of the SP, NCNT, and LCNT were 140.5 mA h g^{-1}, 137 mA h g^{-1}, and 138.5 mA h g^{-1}, respectively at 0.5C.

The capacity retentions of the SP, NCNT, and LCNT were 88.8% (134.9 mA h g^{-1}), 82.6% (127.24 mA h g^{-1}), and 90.9% (134.8 mA h g^{-1}), respectively, after 50 cycles at 0.5C (Fig. 3a). It should be noticed that the capacity retention of LCNT is slightly higher than that of SP, which suggests that the Super P can be replaced with the long CNT (having length in the range of 200–300 μm). This means that the content of the conductive agent can be reduced. Consequently, more amount of active material can be loaded on to the electrode, leading to an increase in energy density. In contrast, the short CNT (having length in the range of 20–30 μm) showed relatively lower capacity retention than the other electrodes. The reason for poor capacity retention of NCNT can be deduced from the impedance analysis

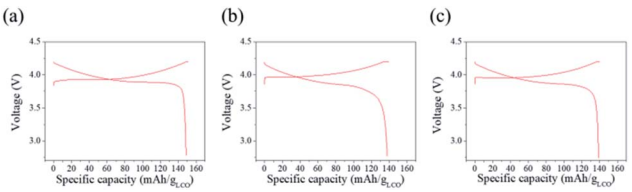

Fig. 2 Galvanostatic charge–discharge tests of half-cells fabricated with (a) SP, (b) NCNT, and (c) LCNT.

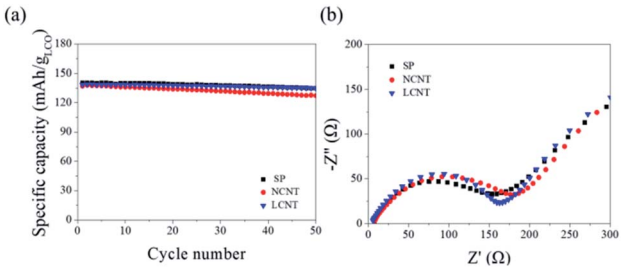

Fig. 3 (a) Cycle performance of SP10, NCT4, and LCNT4 at 0.5C. (b) Nyquist plot of electrodes in the frequency range from 100 kHz to 100 mHz.

(Fig. 3b). The mid-frequency range (100 kHz to 1 Hz) in the impedance spectra is concerned with charge transfer resistance (R_{ct}).[26] The impedance analysis of NCNT showed the highest R_{ct}, which suggests that the length of the short CNT is not enough to form a conductive network for the effective transfer of electrons to the active material at a concentration as low as 4 wt%. This results validate the fact that the higher the aspect ratio of CNTs results in the more effective electrical network in the electrode, resulting in a decrease in the internal resistance of the electrode.

The kinetic properties of LIBs are closely related to the internal resistance of electrode.[27–29] The rate capability test was carried out to explore the effect of the internal resistance electrode on the kinetic properties (Fig. 4). The LCNT exhibited 83 mA h g^{-1} of discharge capacity at 30C. After returning to the current density to 0.1C, the discharge capacity recovered to the similar level of the initial discharge capacity (139.2 mA g h^{-1}), indicating that the LCNT has excellent kinetic properties with a great potential for high power LIBs electrode. On the other hand, SP showed poor rate capability and did not work normally above 15C of current density. In addition, the NCNT showed a very low discharge capacity of 17 mA h g^{-1} at high current density (30C). These results strongly indicate that the aspect ratio of CNTs, which is a conductive agent, greatly affects the kinetic properties of LIB.

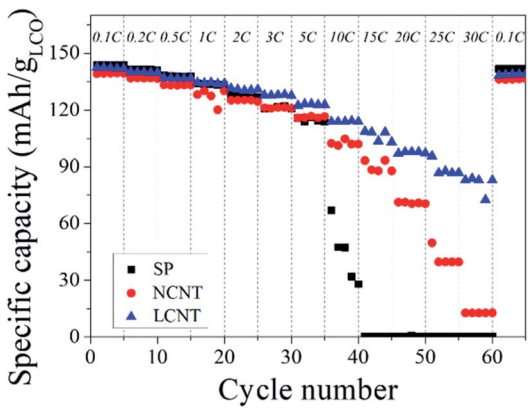

Fig. 4 Rate capability at different current densities (0.1–30C) of the electrodes.

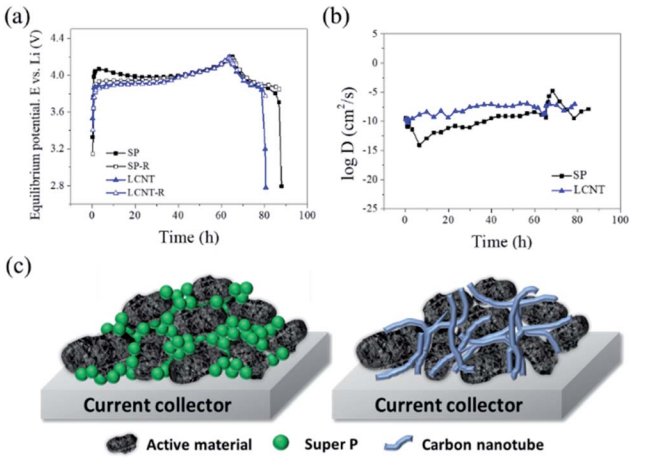

Fig. 5 (a) The GITT curves for SP10 and LCNT4 in the voltage window of 2.8–4.2 V. (b) The Li$^+$ diffusion coefficients of SP10 and LCNT4 calculated from GITT (c) schematic of the structures of the electrodes using Super P and CNT as conductive agent.

Furthermore, it has been known that the kinetic property of the electrode is mainly related to the diffusion of Li$^+$.[30–32] In this study, the conductive agent is a key factor to influence the diffusion of Li$^+$. The GITT analysis was conducted to determine the Li$^+$ diffusion coefficient of two representative SP and LCNT (Fig. 5). The Li$^+$ diffusion coefficient was calculated using the following equation.

$$D = \frac{4}{\pi\tau}\left(\frac{n_m V_m}{S}\right)^2\left(\frac{\Delta E_s}{\Delta E_t}\right)^2$$

where D is Li$^+$ diffusion coefficient, τ (s) is the duration of the current pulse, n_m (mol) is the number of moles, V_m (cm^3 mol^{-1}) is the molar volume of the electrodes and S (cm^2) is the electrode area. ΔE_s (V) is the steady-state voltage change due to the current pulse and ΔE_t (V) is the voltage change during the constant current pulse, eliminating the iR drop.

The iR drop of SP was larger than that of LCNT, which is due to the difference between the charge equilibrium potential and relaxation equilibrium potential (Fig. 5a). The Li$^+$ diffusion coefficient was calculated (Fig. 5b). LCNT shows a 100 times higher Li$^+$ diffusion coefficient than that of SP. From these results, it can be known that LCNT has superior kinetic property than SP, which is in line with the rate capability results discussed (Fig. 4). The outstanding kinetic property of LCNT can be explained in terms of aspect ratio. The conductive agents should build a continuous conductive phase to form an electrically conductive network structure. Since the Super P (0D material) has a low aspect ratio, it seems natural that SP has a large contact resistance. On the other hand, since CNTs have a large aspect ratio, it is easy to form a continuous conductive phase. As a result, it is possible to realize low contact resistance even at low concentrations (Fig. 5c).

4. Conclusion

In summary, we fabricated LCO electrodes using Super P and different lengths of CNTs as conductive agent and investigated

their effects on the kinetic properties of the electrodes. The SP, NCNT, and LCNT showed similar discharge capacity and cycling performance at 0.5C. However, at high current density (30C), the LCNT exhibited superior rate capability and stable performance, while the SP10 and NCNT4 showed poor rate capability. To investigate the effect of the conductive agent on the kinetic properties of the electrodes, Li^+ diffusion coefficient was calculated using GITT analysis. The results indicated that the conductive agent with a high aspect ratio is more favourable for high power LIBs.

Conflicts of interest

There are no conflicts to declare.

Acknowledgements

This work was supported by the National Research Foundation of Korea (NRF) grant funded by the Korea government (MSIT) (NRF-2017R1A5A1015596).

References

1 Y. Tang, Y. Zhang, W. Li, B. Ma and X. Chen, *Chem. Soc. Rev.*, 1995, **44**(17), 5926–5940.
2 K. Zhao, M. Pharr, J. Vlassak and Z. Suo, *J. Appl. Phys.*, 2011, **109**, 016110.
3 B. Liu, J. Zhang, X. Wang, G. Chen, D. Chen, C. Zhou, *et al.*, *Nano Lett.*, 2012, **12**(6), 3005–3011.
4 K. A. Sierros, D. S. Hecht, D. A. Banergee, N. J. Morris, L. Hu, G. C. Irvin, *et al.*, *Thin Solid Films*, 2010, **518**(23), 6977–6983.
5 H. Gwon, J. Hong, H. Kim, D. Seo, S. Jeon and K. Kang, *Energy Environ. Sci.*, 2014, **7**(2), 538–551.
6 J. Tarascon and M. Armand, *Nature*, 2001, **414**(6861), 359–367.
7 S. Lee, H. Song, J. Hwang, S. Kim and Y. Jung, *Carbon Lett.*, 2018, **27**, 98–107.
8 D. Ma, Z. Cao, H. Wang, X. Huang, L. Wang and X. Zhang, *Energy Environ. Sci.*, 2012, **5**(9), 8538–8542.
9 C. Luo, R. Huang, R. Kevorkyants, M. Pavanello, H. He and C. Wang, *Nano Lett.*, 2014, **14**(3), 1127–1133.
10 C. Luo, Y. Zhu, Y. Wen, J. Wang and C. Wang, *Adv. Funct. Mater.*, 2014, **24**(26), 4082–4089.
11 H. Zhang, H. Zhao, M. A. Khan, W. Zou, J. Xu, L. Zhang, *et al.*, *J. Mater. Chem. A*, 2018, **6**(42), 20564–20620.
12 N. Nitta, F. Wu, J. Lee and G. Yushin, *Mater. Today*, 2015, **18**(5), 252–264.
13 B. Lung-Hao Hu, F. Wu, C. Lin, A. Khlobystov and L. Li, *Nat. Commun.*, 2013, **4**(1), 1687.
14 H. Zheng, J. Li, X. Song, G. Liu and V. Battaglia, *Electrochim. Acta*, 2012, **116**(7), 4875–4882.
15 R. Zhao, J. Liu and J. Gu, *Appl. Energy*, 2015, **173**, 29–39.
16 N. Ogihara, Y. Itou, T. Sasaki and Y. Takeuchi, *J. Phys. Chem. C*, 2015, **119**(9), 4612–4619.
17 L. Zhu, J. Xu, Y. Xiu, Y. Sun, D. Hess and C. Wong, *Carbon*, 2006, **44**(2), 253–258.
18 J. Li, P. Ma, W. Chow, C. To, B. Tang and J. Kim, *Adv. Funct. Mater.*, 2007, **17**(16), 3207–3215.
19 F. Du, J. Fischer and K. Winey, *Phys. Rev. B: Condens. Matter Mater. Phys.*, 2005, **72**(12), 121404.
20 Y. Wu, J. Wang, K. Jiang and S. Fan, *Front. Physiol.*, 2014, **9**(3), 351–369.
21 K. Sheem, Y. Lee and H. Lim, *J. Power Sources*, 2006, **158**(2), 1425–1430.
22 K. Wang, Y. Wu, S. Luo, X. He, J. Wang, K. Jiang, *et al.*, *J. Power Sources*, 2013, **233**, 209–215.
23 Y. Wu, H. Wu, S. Luo, K. Wang, F. Zhao, Y. Wei, *et al.*, *RSC Adv.*, 2014, **4**(38), 20010–20016.
24 J. Song, S. Yoon, S. Kim, D. Cho and Y. Jeong, *Chem. Eng. Sci.*, 2013, **104**, 25–31.
25 J. Pikul, H. Gang Zhang, J. Cho, P. Braun and W. King, *Nat. Commun.*, 2013, **4**, 1732.
26 H. Song, S. Jeon and Y. Jeong, *Carbon*, 2019, **147**, 441–450.
27 H. Li, L. Peng, D. Wu, J. Wu, Y. Zhu and X. Hu, *Adv. Energy Mater.*, 2019, **9**(10), 1802930.
28 Y. Zheng, H. Seifert, H. Shi, Y. Zhang, C. Kübel and W. Pfleging, *Electrochim. Acta*, 2019, **317**, 502–508.
29 S. Ahamad and A. Gupta, *Electrochim. Acta*, 2019, **297**, 916–928.
30 Z. Xiao, C. Lei, C. Yu, X. Chen, Z. Zhu, H. Jiang, *et al.*, *Energy Storage Materials*, 2019, **24**, 565–573.
31 Y. Ko, H. Park, B. Lee, Y. Bae, S. Park and K. Kang, *J. Mater. Chem. A*, 2019, **7**(11), 6491–6498.
32 J. Li, T. Zhang, C. Han, H. Li, R. Shi, J. Tong, *et al.*, *J. Mater. Chem. A*, 2019, **7**(2), 455–460.

